Fractal Aperture Distribution of Activated Carbon Fiber and Adsorption Behavior to Low-Density Benzene Steam

Chen Yuhan, Wu Qilin, and Pan Ding

College of Materials, State Key Lab. for Modification of Chemical Fiber and Polymer Materials, Dong Hua University, Shanghai, China

Pan Ning

Center of Soft Fibrous Matters, Dong Hua University, Shanghai, China and Division of Textile and Clothing, Biological and Agricultural Engineering Department, University of California, California, USA

Based on the $J(x)$ fractal distribution function of aperture given by Jaroniec, this article suggests another function $K(x)$, a variant of $J(x)$ but offering new insight. We then use these two functions to characterize three kinds of activated carbon fiber (ACF) of different specific areas. This article also provides the fractal distribution of the aperture and the isotherm of nonpolarity benzene steam on the ACF specimens and the relationship between them.

Keywords   Activated carbon fiber (ACF), fractal, aperture distribution, gas phase adsorption

INTRODUCTION

Activated carbon fiber (ACF) is most used as gas absorbent, especially for low density media[1–3] such as in indoor air depuration, with excellent adsorption efficacy and adsorption kinetics, owing to its great specific area, highly porous structure, a narrow distribution of aperture and short internal path for adsorption and desorption.

This article deals with the methodology in evaluating the performance of given ACS. In characterizing a porous carbon material, one of the key tasks is to describe and assess the size distribution of the micropores, for it largely determines the adsorption effectiveness. The slot-pore is the main source of structural irregularity and energy inhomogeneity. One common way to do this is to use the aperture distribution, but this technique is frequently reported as not accurate enough. So, Pfeifer and Avnir[4] brought the concept of "fractal" into the multipore material to quantitatively describe the structure irregularity and the energy inhomogeneity of the material. It has been reported[5] that for most solids with big specific-area, their fractal dimensions (D) calculated range between 2 and 3, that is, between a planer and a spatial shape. When D is close to 2, the pore tends to be in a plane so its surface is smoother; whereas D is close to 3, the pore is more tortuous and its surface is rougher.

This article proposed a new approach to estimate rayon-based ACF's surface fractal through nitrogen adsorption technique. We first measure the adsorption isotherms of the samples to low-density benzene steam under atmospheric pressure and room temperature so as to establish the relationship between resulting fractal characteristics and the benzene steam adsorption. Then we provide the fractal dimensions of the ACF samples as indicators of the uniformity of the pores in the samples.

THEORETICAL CONSIDERATIONS

Through a theoretical analysis, Jaroniec et al.[7] developed a relationship between the aperture distribution function $J(x)$ and the fractal dimension D for a multipore solid as

$$J(x) = \frac{3 - D}{x_{\max}^{3-D} - x_{\min}^{3-D}} x^{2-D} \qquad [1]$$

where, x is the aperture half-width, and $x_{\min}$, $x_{\max}$ represent the minimum and maximum x values. For convenience, their derivation process is briefly provided below.

According to the micropore adsorption theory, the adsorption isotherm for a porous material can be described as:

$$\Theta = \int \theta J(x) dx \qquad [2]$$

where,

Θ—the material adsorption isotherm

θ—the partial adsorption isotherm for an aperture size x

$J(x)$—micropore aperture distribution function within the boundary (x_{min}, x_{max})

For a microporous solid with a fractal dimension D, the aperture distribution function $J(x)$ fits a proportional relationship:[4]

$$J(x) = \rho x^{2-D} \qquad [3]$$

Where ρ is a proportional constant, and can be determined by

$$\int_{x_{min}}^{x_{max}} J(x)dx = 1 \qquad [4]$$

through three Equations (1), (3) and (4), we can derive the three parameters.

Besides, we can also get the mean aperture width related with $J(x)$ as:[8]

$$\bar{x} = x_{min}\left(\frac{3-D}{4-D}\right)\left(\frac{r^{4-D}-1}{r^{3-D}-1}\right) \qquad [5]$$

where $r = x_{max}/x_{min}$. If we substitute $\Theta = V/V_0$ into formula (2), then

$$\int_{x_{min}}^{x_{max}} V_0 \theta J(x)dx = V \qquad [6]$$

where,

V_0—total pore volume taken by the absorbent
V—total pore volume available in the material.

Introduce

$$K(x) = V_0 J(x) \qquad [7]$$

then from Equation (4)

$$\int_{x_{min}}^{x_{max}} K(x)dx = V_0 \qquad [7b]$$

We, thus, can get the modified fractal aperture distribution of the solid with fractal micropores:

$$K(x) = V_0 \frac{3-D}{x_{max}^{3-D} - x_{min}^{3-D}} x^{2-D} \qquad [8]$$

Although there is no substantial difference between Equations (1) and (8), Equation (1) shows the ratios of each size x of the pores in the material, whereas Equation (8) offers the volume of each size of the pores taken by the absorbent; this difference is clearly shown in Equation (7).

Furthermore, by comparing Equations (4), (7), and (8), we can find that the dimensional unit for $J(x)$ is L^{-1} whereas for $K(x)$ is L^2. The unit renders a geometrical meaning of area to $K(x)$, which is often advantageous when coming to deal with absorption, for it is easier to associate absorption to pore area that to a reciprocal length. We use both functions to analyze the adsorption experiments below.

THE EXPERIMENTAL CHARACTERIZATION

Three kinds of rayon-based ACFs with different specific areas are selected and marked as A1, A2 and A3. The isothermal adsorption experiments were conducted at 77°K in a 360CX nitrogen adsorption instrument, and the deaerating process lasted 12 hours, at 250°K, and pressure $6e^{-5} \times 13.332$ pa.

Samples of $10 \sim 20$ mg were put on the plate of a thermogravimetry analysis instrument, blown by $60\,cm^3/minute$ high purity nitrogen of 25°K for a given period of time before reducing its concentration by diluting with the standard purity nitrogen.

RESULTS AND DISCUSSION

The Aperture and Fractal Characteristics of the ACF Samples

Our N_2 adsorption isotherm[6] results show that all three samples are highly microporous. From the pore structure parameters (Table 1), we see a direct connection between the specific area and the micropore volume, as expected. If using the H-K method[6] to analyze the micropores in the samples, the specific area of A1 is the smallest resulting from the lest volume of micropore. A3 is the greatest in both values and A2 lies in between. Again, the ranking order for the specific area corresponds to that of the pore volume.

In terms of the pore size itself, there are two parameters; the H-K average aperture and the $J(x)$ average half-width. For the same samples, the two parameters appear to offer slightly different results. According to the H-K average aperture, the pore size ranking is A3> A2 > A1; whereas in the $J(x)$ average, it becomes A2 > A3 > A1. Nevertheless, the difference between A2 and A3 in H-K average case is too small to claim that the two methods are not in agreement.

There are several ways to measure the value of the fractal dimension D, an indicator of the smoothness of the pores, such as adsorption method, X-ray scattering method, STM method, etc. In this article, we used the nitrogen adsorption method to obtain the sample fractal dimensions as shown in

TABLE 1
The sample aperture and fractal characteristics

Sample	A1	A2	A3
Specific area, $m^2\,g^{-1}$	640	1460	1680
Volume of micropore, $cm^3\,g^{-1}$	0.271	0.451	0.546
Fractal dimension D	2.84	2.26	2.56
H-K average aperture, nm	0.70	0.96	0.95
$J(x)$ average half-width of slot, nm	0.42	0.51	0.46

Table 1. It is seen that A1 has pores that are the roughest as reflected by the greatest D value, followed by A3 and then A2.

According to reference [8], we set $x_{max} = 1.0$ nm, $x_{min} = 0.1$ nm. Bringing the D values in Table 1 into Equations (1) and (8) respectively, we get the corresponding fractal aperture distributions of the three samples of $J(x)$ shown in Fig. 1 and $K(x)$ in Figs. 2. Note that the $K(x)$ curves are related to $J(x)$, D and V_0.

As seen in the Figures 1–3, $J(x)$ and $K(x)$ are both monotonically decreasing functions, meaning there are more smaller pores than the larger ones in all three samples.

As mentioned before, $J(x)$ heuristically reflects the ratio of the micropores in different sizes in the samples. A greater D value usually indicates a higher ratio of smaller size micropores, and, thus, a steeper slope of the $J(x)$ curve. Conversely a smaller D value and hence a more even $J(x)$ curve indicate more uniform structural regularity and energy homogeneity of the sample.

For the $K(x)$ curve on the other hand, its values are more closely associated with the adsorbate volume absorbed by an absorbent.

The Adsorption of ACF to Low-Density Benzene Steam

Because of its excellent adsorption property, ACF is very effective in controlling the quality of indoor air. We focus in this study on the adsorption efficacy of the ACF to gaseous benzene under room temperature (25°C) and atmosphere pressure, for benzene is a nonpolarity substance and is chemically inertia toward the functional groups on the surface of the ACF; thus, more resistant to be absorbed. In other words, using benzene gas as a tracer can magnify the resolution of our method.

Since the adsorption of the ACF to low-concentration benzene gas is very slow, for example, under the concentration of 50×10^{-6}, it took us about 20–30 hours to complete one experiment; we limited our tests over the concentration range of $50 \times 10^{-6} \sim 1000 \times 10^{-6}$. The testing results are illustrated in Figure 3.

From the experimental data in Figure 3, samples with greater specific area yield higher adsorption volume, that is,
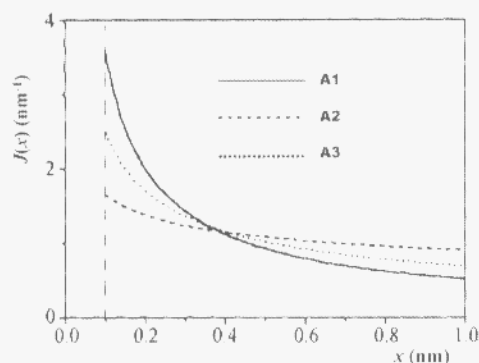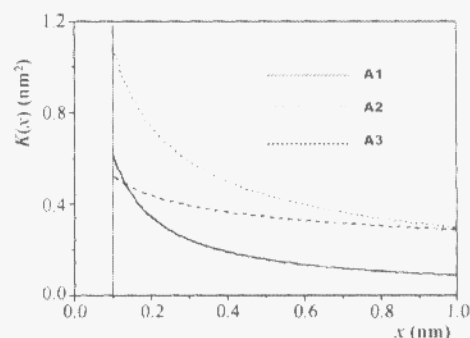

FIG. 2. The $K(x)$ fractal aperture distributions for three samples.

$A3 > A2 > A1$. Because the specific area of A2 is very close to that of A3, their adsorption isotherms are also near to each other. On the other hand, A1 has the smallest micropore volume so its adsorption isotherm is flatter, or its adsorption rate is slower and efficacy is lower.

If we compare Figure 3 to the $K(x)$ curves in Figure 2 at the pore size range of the three samples from 0.7 nm to 0.96 nm, we will find that for the three samples, the $K(x)$ ranking in Figure 2 is identical to that of the adsorption capacity in Figure 3. It is not the case when comparing with $J(x)$ in Figure 1.

Next, we used the Dubinin-Radushkevich formula[11] to fit the experimental data in Figure 3 and extrapolate the curves for the three samples over a wider benzene concentration range of $0.1 \times 10^{-6} \sim 10000 \times 10^{-6}$ as in Figure 3. It now shows that when the benzene concentration is very low $< 1.0 \times 10^{-6}$, A1 turns out to show the highest adsorption capacity of the three. If this extrapolation holds, a possible explanation would be that, the small pores become more effective in adsorbing the benzene gas at very low concentration, as if when not crowded, the gas molecules have higher changes to interact with more, large or small, pores so as to be trapped. In other words, the interaction energy between the solid molecules and gas molecules is

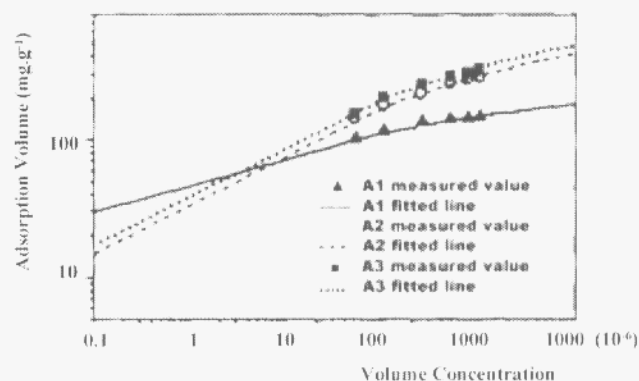FIG. 1. The $J(x)$ fractal aperture distributions for three samples.

FIG. 3. The testing data and fitted lines of ACF adsorptions to benzene steam.

enhanced at extremely low gas concentration and/or smaller aperture pores.

Now if we compare the fitted lines in Figure 3 to the $J(x)$ curves in Figure 1, we can see that for the same sample size ranges 0.7 nm to 0.96 nm, the reversed $J(x)$ distribution (or $1/J(x)$) ranking now shows consistence with that of their adsorption volumes, that is, A1 > A3 > A2, which, in turn, is consistent with the ranking of their fractal dimension D values. So we can speculate that at relatively high concentration of benzene gas, $K(x)$ distribution offers a better prediction of the ACF adsorption capacity, whereas in extremely low concentration case, both $J(x)$ and D are more useful.

CONCLUSIONS

Based on the present study, the following conclusions can be drawn:

(1) $J(x)$ function describes the ratio, and the modified $K(x)$ function does the relative volume, of the different aperture sizes in a porous material.
(2) For the same pore volume, when the benzene concentration in the air is relatively high, the ACF with more bigger pores exhibits higher adsorption power. Yet, at extremely low concentration, it's the ACF with more smaller pores that works more effectively.
(3) When the benzene concentration in the air is high, $J(x)$ reflects the adsorption capacity of ACF more accurately; whereas $K(x)$ and the fractal dimension D become better indicators at very low benzene concentration case.

ACKNOWLEDGEMENT

REFERENCES

[1] Foster, K.L., Fuerman, R.G., Economy, J., et al. (1992) Adsorption characteristics of trace volatile organic compounds in gas streams onto activated carbon fibers. *Chemistry of Materials*, 4 (5): 1068–1073.
[2] Huang, Z.H., Kang, F.Y., and Liang, K.M. (2000) Adsorption of VOCs on viscose rayon based activated carbon fiber. In *The Proceedings of 1st World Conference on Carbon, 2000*, Scharff, P. (ed.), German Carbon Group: Berlin, 143–144.
[3] Suzuki, M. (1994) Activated carbon fiber: fundamentals and applications. *Carbon*, 32 (4): 577–586.
[4] Pfeifer, P. and Avnir, D. (1983) Chemistry in non-integer dimensions between two and three. I. Fractal theory of heterogeneous surfaces. *J. Chem Phys*, 79: 3558–3565.
[5] Ismail, I.M.K. and Pfeifer, P. (1994) Fractal analysis and surface roughness of nonporous carbon fibers and carbon blacks. *Langmuir*, 10: 1532–1538.
[6] Dreisbach, F., Staudt, R., and Keller, J.U. (1999) High pressure adsorption data of methane, nitrogen, carbon dioxide and their binary and ternary mixtures on activated carbon. *Adsorption*, 5: 215–227.
[7] Jaroniec, M., Lu, X., Madey, R., and Avnir, D. (1990) Thermodynamics of gas adsorption on fractal surfaces of heterogeneous microporous solids. *J. Chemical Physics*, 92: 7589–7595.
[8] Jaroniec, M. and Gilpin, R.K. (1993) Correlation between microporosity and fractal dimension of active carbons. *Carbon*, 31 (2): 325–331.
[9] Gregg, S.J. and Sing, K.S.W. (1982) *Adsorption, Surface Area and Porosity*; Academic Press: London, 218–257.
[10] Kaneko, K. and Setoyama, S.T. (1994) Ultramicropore characterization by the adsorption. *Stud. Surf Sci Catal.*, 97: 593–602.
[11] Dubinin, M.M. (1989) Fundamentals of the theory of adsorption in micropores of carbon adsorbents: Characteristics of their adsorption properties and microporous structures. *Carbon*, 27: 457–467.